

# Effect of Geometry and Surface Properties of Silicates on Nanostructuring of Suspension in Precursors of an Epoxy/Amine Network

Amar Boukerrou,<sup>1</sup> Jannick Duchet,<sup>2</sup> Said Fellahi,<sup>3</sup> Henry Sautereau<sup>2</sup>

<sup>1</sup>Laboratoire des Matériaux Organiques, Université de Béjaia, Algérie

<sup>2</sup>Laboratoire des Matériaux Macromoléculaires, IMP UMR#5627, INSA de Lyon, Bâtiment Jules Verne, 20 avenue Albert Einstein, 69621 Villeurbanne Cedex, France

<sup>3</sup>Département de Génie des Polymères, Institut Algérien du pétrole, 35000 Boumerdès, Algérie

Received 29 November 2005; accepted 17 January 2006

DOI 10.1002/app.24185

Published online in Wiley InterScience (www.interscience.wiley.com).

**ABSTRACT:** Several lamellar silicates (Montmorillonite, Hectorite, Mica) showing different host structures and aspect ratios were modified with octadecylammonium ions by a cationic exchange process. The resulting organoclays were characterized using thermal gravimetric analysis and X-ray diffraction, which allowed us to estimate the amount of surfactants within the organoclays and their organization in the interlamellar spacing. Some local pseudo-organizations were found and checked by differential scanning calorimetry (DSC). The interactions of organophilic silicates were evaluated, without any shear, with the precursors of a rubbery epoxy/amine network. These silicate/monomers interactions were monitored via the measurements of the inter-

lamellar swelling, the surface energies and the physical gel formation. The organoclays used form gels in the monomers above the percolation threshold if no shear is applied and present a gel/sol transition at a critical shear stress. Gel strength determined from storage modulus and viscosity values determined at high shear rates reveal different organizations of clay in the monomers depending on the silicate aspect ratio and silicate/monomers interactions. © 2006 Wiley Periodicals, Inc. *J Appl Polym Sci* 102: 1380–1390, 2006

**Key words:** lamellar silicate; epoxy-amine; suspension; dispersion; physical gel

## INTRODUCTION

Polymer-layered silicate nanocomposites have attracted a great deal of attention both in academic and industrial fields since many potential improvements are waited by introducing layered silicates in polymers: increase of mechanical properties,<sup>1,2</sup> improvement of barrier properties and flame retardation,<sup>3–5</sup> and better dimensional and thermal stability.<sup>6</sup> But, the dispersion state is the key parameter that must be tailored because it is the spatial organization of inorganic clay sheets in the polymer matrix that govern the final properties of material. An homogeneous dispersion without aggregation of elementary nanolayers or only a few platelets tactoids is researched to develop the highest amount of interfacial zone to favor the interactions with the dispersion medium. This can be addressed by modifying the clay so that the clay surface becomes organophilic. Clays such as montmorillonites have a remarkable ions exchanging property. Their structure consists of two fused silica tetrahedral sheets sandwiching an edge-shared octahedral sheet.

In the tetrahedral sheet,  $\text{Si}^{4+}$  may be replaced by trivalent cations ( $\text{Al}^{3+}$ ), or divalent cations ( $\text{Mg}^{2+}$  or  $\text{Fe}^{2+}$ ) may replace  $\text{Al}^{3+}$  in the octahedral sheet. The isomorphous substitution will result in positive charge deficiency on the surface of the clay. This lack is compensated by cations such as  $\text{Ca}^{2+}$  and  $\text{Na}^{+}$  situated in the interlayers. An exchange of these cations with alkylammonium ions renders the clay organophilic and lowers its surface energy, leading to an easier organic chains intercalation between clay layers. The cation-exchange capacity (CEC) allows quantify the total amount of exchangeable cations in the clay interlayer, expressed in milliequivalents per hundred grams of dry clay. This property is strongly dependent on the isomorphous substitutions in the tetrahedral and octahedral layers.

Organophilic clays are known for their absorption capacities and their ability for swelling and thixotropic gel formation in organic media.<sup>7,8</sup> The swelling of untreated sodic montmorillonite in water was considered as a model for many years because of its high swelling capacity and its ability to form stable suspensions.<sup>9</sup> If the concentration of clay is enough, clay platelets association induces the formation of a continuous structure leading to a gel-like behavior. Despite many investigations on the subject, the swelling

Correspondence to: A. Boukerrou (aboukerrou@yahoo.fr).

of organophilic clays in organic media is not clearly understood. Gherardi<sup>10</sup> has found that the physical gelation process in organic media was a complex phenomenon affected by several parameters such as the nature of clay, the nature of modifying ions, and dielectric constant of the organic medium. Indeed, Moraru<sup>11</sup> observed for the same alkyl chain length that gel formed is stiffer when the organic chains contain aromatic groups whereas alkylammonium derivatives display a lower swelling ability because of the strong bridging between layers. The organic medium can be either an organic solvent in the case of nanocomposite processing from a polymer solution or a reactive solvent like a monomer in the case of nanocomposite processing from *in situ* polymerization of monomers. Recently, Burgentzlé et al.<sup>12</sup> have shown that the physical gel is formed by percolation of 3–4 platelets-based tactoids in an appropriate organic solvent even if the platelets are not necessarily swollen in the interplatelet galleries. No correlation between interlayer swelling and macroscopic swelling was put into evidence. On the one hand, the macroscopic swelling depends on chemical interactions. Very organophilic nanoclays as those modified by quaternary ammonium ions containing benzyl or/and ditallow groups form a gel with aromatic or dispersive solvents. However nanoclays both polar and organophilic require a solvent showing this dual character to form a gel. On the other hand, the nanoscopic swelling between platelets is favored when the solvent used is both polar and organophilic, i.e., possess a high surface tension fulfilling the following condition:  $\gamma_{\text{solvent}} \geq \gamma_{\text{ion}}$ . High surface energy solvents are effective for gelation and the balance between the hydrophilic and hydrophobic part of the solvent molecules is the key of the dispersion of the silicate (polar) platelets modified by alkylammonium ions (apolar or less polar than the silicate platelets). These results are in agreement with Jordan's<sup>13</sup> conclusions, who demonstrated that a high adsorption energy on silicates and a solvation energy of the intercalated omnium ions are both conditions to fulfill to assure swelling process at the scale of the platelets, and not strongly at the macroscopic scale.

Owing to the multiscale organization of nanoclays (i.e., individual nanolayers), association of these ones in tactoids, and possible formation of nanofillers network in the organic medium, it is very important to associate several analytical methods to investigate over different observation scale ranges. Recently, Krishnamoorti and Yurekli<sup>14</sup> have proved that viscoelastic measurements were highly sensitive to the nanoscale and mesoscale structure of the nanocomposite suspensions and appear to be a powerful method to probe the underlying structure of these materials. The gel strength increases gradually with structure changes linked to dispersion state, from the

well dispersed state to the flocculated state and then the aggregated state. In a previous work,<sup>15</sup> we have shown that the organoclays used formed physical gels in the monomers of an epoxy-amine network above the percolation threshold (lower than 1 vol %) if no shear was applied. The gel viscoelastic properties are linked to the nanometric state of dispersion and reveal the existence of two different organizations depending on organoclay/monomer interactions:

- i. When the clay shows good interactions with the monomer, a significant swelling of the clay galleries by monomer is obtained. These swollen particules lead to formation of weak gels.
- ii. When the clay develops poor interactions with the monomer, the clay tends to reduce its exchange surface with the monomer and leads to a stiff connected gel.

In this work, the objective is to understand the effect of aspect ratio and chemical modifications of the clays on the interactions between these organoclays and the precursors of an epoxy/amine network.

These silicate/monomers interactions, which govern the compatibility and dispersion of nanoclays in the organic medium, were measured at three scale levels: (i) at nanometer-scale by measuring the interlamellar swelling, (ii) at the micrometric scale from rheological analysis of clay/monomer suspensions, and (iii) at the macroscopic scale by swelling ratio measurements. Three layered silicates with different host structures and surface properties were studied: (i) an algerian bentonite, which is an aluminous silicate (ii) a synthetic fluoromica, which is rather a magnesian silicate; (iii) an hectorite, which is a synthetic sodic silicate containing mainly magnesium and lithium.

## EXPERIMENTAL

### Materials

The three studied nanofillers are a natural algerian bentonite (called MMT) supplied by Entreprise Nationale des Corps Gras de Béjaia (Algeria), a synthetic hectorite (called HECT) supplied by Süd-Chemie (Germany), whose trade name is Optigel SH, and a synthetic fluorosilicate (called MICA) provided by Coop Chemicals (Japan), whose trade name is SO-MASIF ME100. The organic medium is each precursor of the epoxy/amine network: (i) the epoxy prepolymer is a diglycidyl ether of bisphenol A with  $\bar{n} = 0.15$  and  $M_{\bar{n}} = 3826$  g/mol, further denoted as DGEBA (LY556 from Vantico, France), (ii) the curing agent is an aliphatic diamine with a polypropylene backbone with  $M_{\bar{n}} = 1970$  g/mol, further denoted as D2000 (Jeffamine D2000 from Huntsman, Belgium).

The silicates were incorporated in DGEBA and D2000 with a nanofiller ratio of 5 phr by careful hand mixing for 10 min at 80°C. This temperature was chosen because the curing of the reactive epoxy/amine system takes place at 80°C.

### Organoclay preparation

The method for organoclay preparation is similar to one used by Le Pluart et al.<sup>16</sup> The silicates were exchanged with octadecylammonium ions at 80°C with an amine/clay ratio corresponding to 2CEC. The octadecylamine (0.2 mol) was dissolved in 20 L of 0.01N hydrochloric acid solution (based on deionized water). The solution was stirred at 80°C for 3 h. Then 100 g of clay were added to the solution, which was then stirred at the same temperature for three more hours. The solution was filtered and the silicates were further washed six times more with hot deionized water and one time with a hot ethanol:water (1 : 1) mixture so that no chloride was detected upon adding 0.1M aqueous AgNO<sub>3</sub>. The resulting organoclay was then dried at 85°C for 36 h and kept dry in a vacuum box. After modification, the organoclays will be called MMTC18, HECTC18, and MICAC18.

### Characterization of surface modification

Many analysis tools were used to characterize the lamellar silicates surface modification.

### Surface analysis

Wettability measurements were performed on a GBX device from the sessile drop method. From contact angle measurements with water and diiodomethane as test liquids, the surface energies were determined by using Owens and Wendt theory.

### Physicochemical analysis

Elemental atomic analysis measurements were performed to determine silicates composition.

FTIR spectra were obtained using a Nicolet 710 FTIR spectrometer. 3 mg of each sample previously dried at 150°C were mixed with 160 mg of KBr and pressed on disks.

Thermogravimetric analyses were carried out using a TGA2950 apparatus from TA Instruments. The samples were heated from 25 to 800°C at a scanning rate of 20 K/min under helium atmosphere to evaluate the amount of intercalated alkylammonium ions.

### Structural analysis

Wide Angle X-Ray Diffraction measurements (WAXD) were performed using a Siemens D500 diffractometer

equipped with a back monochromator and a copper cathode as the X-Ray source ( $\lambda = 0.154$  nm). Analyses were performed both on the montmorillonite powder and on the swollen part taken from the clay/solvent(s) suspensions. The  $2\theta$  angles were varied between 1 and 10° to measure the  $d_{001}$ -spacing of the modified montmorillonite. The  $d_{001}$  distance is referred as a peak on intensity versus  $2\theta$  plot. A disappearance of the peak indicates that the nanoclays are well dispersed in the organic medium, i.e., there is no repeated distance of oriented silicate platelets in the investigated range of distances. This state is denoted as "exfoliated." However, a shift of the peak of the neat montmorillonite to lower  $2\theta$  values indicates the increase of the  $d_{001}$ -spacing corresponding to the intercalation of the organic molecules into the interplatelet galleries.

The organization between platelets of the alkyl-ammonium ions via Van der Waals interactions was evidenced by using Differential Scanning Calorimetry from Mettler Co. TA2000. DSC measurements were performed under nitrogen atmosphere with a heating rate of 10 K/min. A crystallinity rate (%) of alkylammonium ions was evaluated using the following equation:

$$\chi = 100 \times (\Delta H_{\text{ions}} / \Delta H_{\text{PE100}}) \quad (1)$$

where  $\Delta H_{\text{PE100}}$  is the melting enthalpy of a 100% crystalline polyethylene (280 J/g).<sup>17</sup>

### Silicate/monomer interactions characterization

#### Rheological analysis

The rheological properties of the silicate/monomer suspensions at 5 phr were carried out on a Thermal Analysis AR1000 rheometer, with a cone-plate geometry (diameter 60 mm and 0.02 rad). A 30 min rest time was applied to samples after setting between cone and plate so that the suspensions relax and are in the same reference state before shearing. All measurements were performed at 80°C, which corresponds to the curing temperature of the epoxy/amine network.

The evolution of the storage shear modulus,  $G'$ , at a frequency of 1 rad/s, as function of the amplitude of the dynamic strain was recorded, from 0.01 to 100%, to check if the suspensions behave as gels up to a critical strain corresponding to the end of the linear domain.

The evolution of the storage shear modulus,  $G'$ , at a frequency of 1 rad/s, was also analyzed as a function of an applied shear stress  $\tau$ , from 0.01 to 100 Pa. For each system the flow stress, denoted  $\tau_{\text{stress at break}}$  for which the rheological behavior of the material becomes liquid-like (i.e., for a 90° loss angle) was determined.

**TABLE I**  
**Chemical Composition of Silicates Determined by Elemental Analysis**

Name	C (%)	N (%)	O (%)	Si (%)	Al (%)	Fe (%)	Ca (%)	Mg (%)	Na (%)	K (%)	Li (%)	F (%)
MMT	<0.20	<0.10	37.28	26.97	7.22	1.10	0.30	1.73	0.87	1.51	150 (ppm)	120 (ppm)
HECT	<0.20	0.10	42.09	24.36	430 (ppm)	100 (ppm)	320 (ppm)	15.82	1.60	200 (ppm)	0.27	440 (ppm)
MICA	<0.20	<0.10	30.30	27.79	0.25	490 (ppm)	320 (ppm)	16.58	3.85	80 (ppm)	<0.10 (ppm)	4.12

**Free swelling**

To characterize the interactions at a macroscopic scale, 5 g of organophilic clays were slowly introduced in a graduated test tube containing 100 mL of monomer, DGEBA or JEFFAMINE D2000. Without any mixing, only the wetting of the nanoclays by monomer is searched. The sediment volume of swollen nanoclays was measured after 24 h at room temperature. This process will be denoted later as free swelling. To compare the different swollen volumes,  $V_s$ , defined as the volume of the slurry, it is necessary to take into account the volume of the dry powder,  $V_c$ . The free swelling factor,  $S$ , can be calculated from the following equation

$$S = (V_s - V_c) / V_c \quad (2)$$

$S = 0$  means that the nanoclays are not swollen by the organic medium whereas for  $S = 1$ , the volume is twice the initial volume of the nanoclay powder.

**RESULTS AND DISCUSSION**

**Initial silicate structure and chemical composition analysis**

The three fillers are mainly made up of silica but are different by the oxides content as checked in Table I. MMT is an aluminous silicate containing Fe, Ca, Mg, Na, and K. The infra-red spectrum exhibits both bands at 3631 and 913  $\text{cm}^{-1}$  characteristic of Al—Al—OH groups.<sup>10</sup> On the other hand, HECT and MICA are primarily silicates based on sodium and magnesium characterized by both Mg—Mg—OH bands at 3683 and 652  $\text{cm}^{-1}$  on the IR spectrum. From elemental analysis and X ray diffraction data, the chemical formula can be determined:  $\text{Na}_{0.19}\text{K}_{0.20}\text{Ca}_{0.04}(\text{Mg}_{0.36}\text{Fe}_{0.10}\text{Al}_{1.44})\text{Si}_4\text{O}_{10}(\text{OH})_2$ ,  $\text{Na}_{0.32}(\text{Mg}_{2.82}\text{Li}_{0.18})\text{Si}_4\text{O}_{10}(\text{OH})_2$ , and  $\text{Na}_{1.08}\text{Mg}_{1.96}\text{Al}_{0.13}\text{Si}_4\text{O}_{10}\text{F}_2$  for the bentonite (MMT), hectorite (HECT), and MICA, respectively. These formula are quite in agreement with those reported in the literature.<sup>18–20</sup>

The X-ray diffraction spectra gathered in Figure 1 already reveal the differences of purity and crystalline organization between the three silicates. The first peak located on the spectrum characterizes the repetition of platelet in the direction, (001) i.e.,  $d$ -spacing and the others peaks allow to identify the silicate host structure and the impurities. The strong and well resolved

reflections of MICA prove the high purity and the ordered structure on long distances of this synthetic silicate [Fig. 1(c)]. The natural silicate, i.e., montmoril-

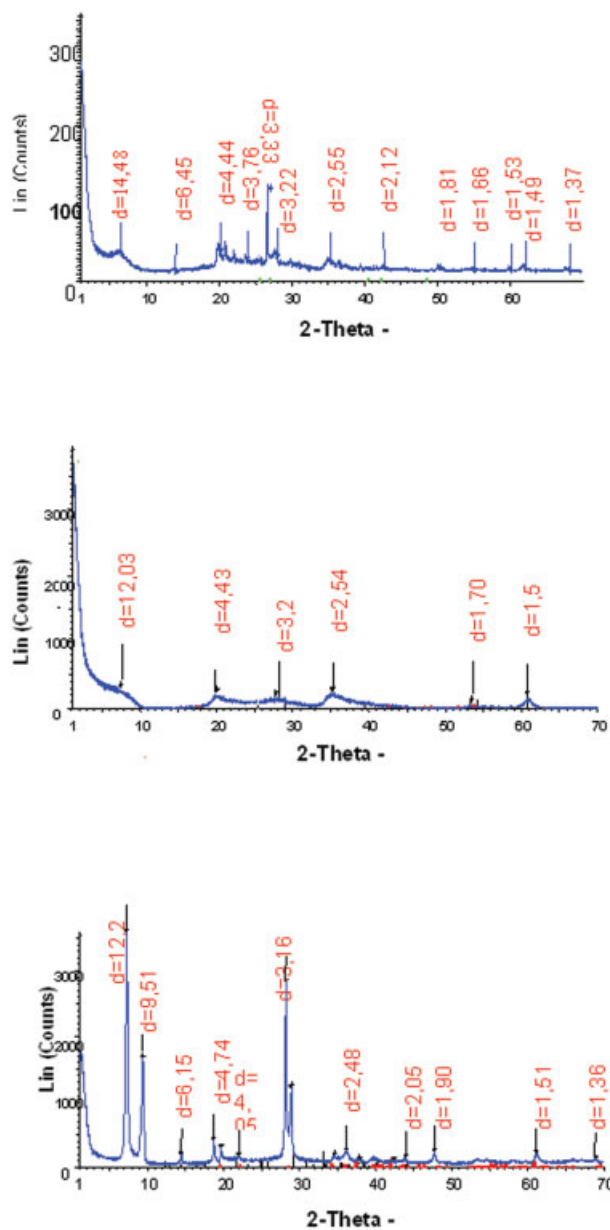


**Figure 1** XRD Spectra of three pristine lamellar silicates: (a) MMT, (b) HECT, and (c) MICA. [Color figure can be viewed in the online issue, which is available at [www.interscience.wiley.com](http://www.interscience.wiley.com).]

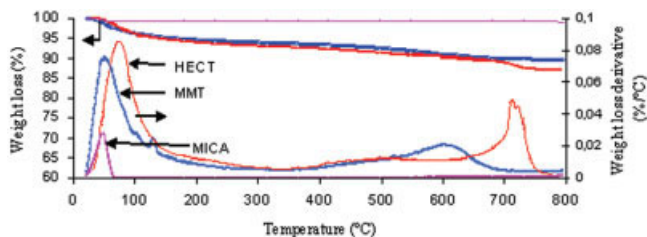


**Figure 2** Weight loss and weight derivatives of three pristine lamellar silicates: MMT, HECT, and MICA. [Color figure can be viewed in the online issue, which is available at [www.interscience.wiley.com](http://www.interscience.wiley.com).]

lonite shows a peak characteristic of a distance at  $d_{060} = 1.49 \text{ \AA}$ . checking that MMT is a dioctaedral clay where 2 sites on 3 in the octahedral layer are occupied by cations. Its WAXD spectrum shows much less pronounced diffraction peaks, indicating a poorer crystalline organization of platelets on long distances. This natural silicate contains more impurities like quartz identified by the peak situated at  $3.33 \text{ \AA}$ . [Fig. 1(a)]. Although hectorite is a synthetic silicate, the diffraction peaks are less resolved. The shoulder at  $12.03 \text{ \AA}$  reveals the lack of platelet organization on long distances. The distance at  $1.52 \text{ \AA}$  reveals that all the octahedral sites are occupied by cations, hectorite is a trioctaedral clay. Usually Montmorillonite has one or two water layers, absorbed on the platelet surface according to the capacity of the intergallery cations to be hydrated. One also considers that each water layer increases the  $d$ -spacing of  $3 \text{ \AA}$ . In this case, we can say that MMT, which contains both calcium and sodium ions has an additional water layer when compared with both sodic silicate others, since the X-Ray spectrum shows the first peak characteristic of the distance  $d_{001}$  corresponding to the hydrated gallery at  $14.5 \text{ \AA}$  for MMT against  $12 \text{ \AA}$  for MICA and HECT. The synthetic silicates contain only one water layer against two layers for the natural silicate. Drying of silicates in an oven at  $80^\circ\text{C}$  during 36 h is not enough to remove water since any modification on the WAXD spectra cannot be put into evidence. So drying in these conditions does not influence the crystallographic structure of clays. These results are in conformity with the work of Xie et al.<sup>21</sup>, who found that the  $d$ -spacing  $d_{001}$  decreases from  $15 \text{ \AA}$  for a calcic silicate or  $11\text{--}12.5 \text{ \AA}$  for a sodic silicate, to  $9.5 \text{ \AA}$  after drying at  $500^\circ\text{C}$  to remove the linked water.

The thermal stability of clays analyzed by TGA from the weight loss derivative ( $dm/dT$ ) as a function of the temperature, is reported in Figure 2. For MMT and HECT, three areas of weight loss on DTG curves can be observed.<sup>22</sup> The first volatile departure at temperatures lower than  $150^\circ\text{C}$  is associated with the vaporization of free water (between pores and aggregates). The second area is attributed to departure of interca-

**TABLE II**  
Polar and Dispersive Components of Surface Energy of Clays after Modification with Alkylammonium Ions

Silicates	$\gamma_p$ (mJ/m <sup>2</sup> )	$\gamma_d$ (mJ/m <sup>2</sup> )	$\gamma_T$ (mJ/m <sup>2</sup> )
MMTC18	4.2	29.5	33.7
HECTC18	2.1	28.1	30.2
MICAC18	0.8	31.3	32.1

lated water on a temperature range included between  $350$  and  $670^\circ\text{C}$ , and for higher temperatures between  $650$  and  $750^\circ\text{C}$ , the dehydroxylation of silicates is observed. On the thermogram of the mica, only one weight loss at a temperature lower than  $100^\circ\text{C}$  related to physisorbed water is determined.

### Organophilic modification of nanosilicates

After the cationic exchange, the silicate surface properties are modified. The organoclays display a higher dispersive component and a lower polar component of the surface energy, as shown by the values calculated from the contact angle measurements using the Owens–Wendt theory<sup>23</sup> (Table II). MICAC18, which is the silicate containing less water (Table III), has the lowest polar component ( $\gamma_p$ ) proving its hydrophobic character quite similar to a polyolefin one since its dispersive component ( $\gamma_d$ ) is about  $31 \text{ J m}^{-2}$ . On the other hand, HECTC18 and MMTC18 present a dispersive component ( $\gamma_d$ ) rather similar to wax one. MMTC18 shows the highest polar component ( $\gamma_p$ ) which is significant of the presence of more polar groups, such as hydroxyl groups situated on platelets edges. Results of surface energy of those organoclays are very close to those obtained by Le Pluart et al.<sup>16</sup> for natural montmorillonites modified by octadecylammonium ions.

WAXD spectra of the three modified samples shown in Figure 3 reveal that the basal spacing has been increased from  $14.5$  and  $12.3 \text{ \AA}$  to  $28.6$  and  $25.3 \text{ \AA}$  for MMTC18 and MICAC18 respectively, demonstrating the intercalation of long chain octadecylammonium ions between the platelets. The spectrum of MICA shows a large peak significant of interlamellar spacing distribution between  $28$  and  $17 \text{ \AA}$ . The organo-

**TABLE III**  
Determination of the Amount of Intercalated Or Physisorbed Ions ( $v = 20 \text{ K min}^{-1}$ ) by TGA

Sample	% By weight in the sample			
	Water	Physisorbed ions	Intercalated ions	Deduced CEC (meq/100 g)
MMTC18	0.47	12.69	18.35	90
HECT C18	2.39	15.38	22.43	120
MICA C18	0.20	19.71	14.27	70

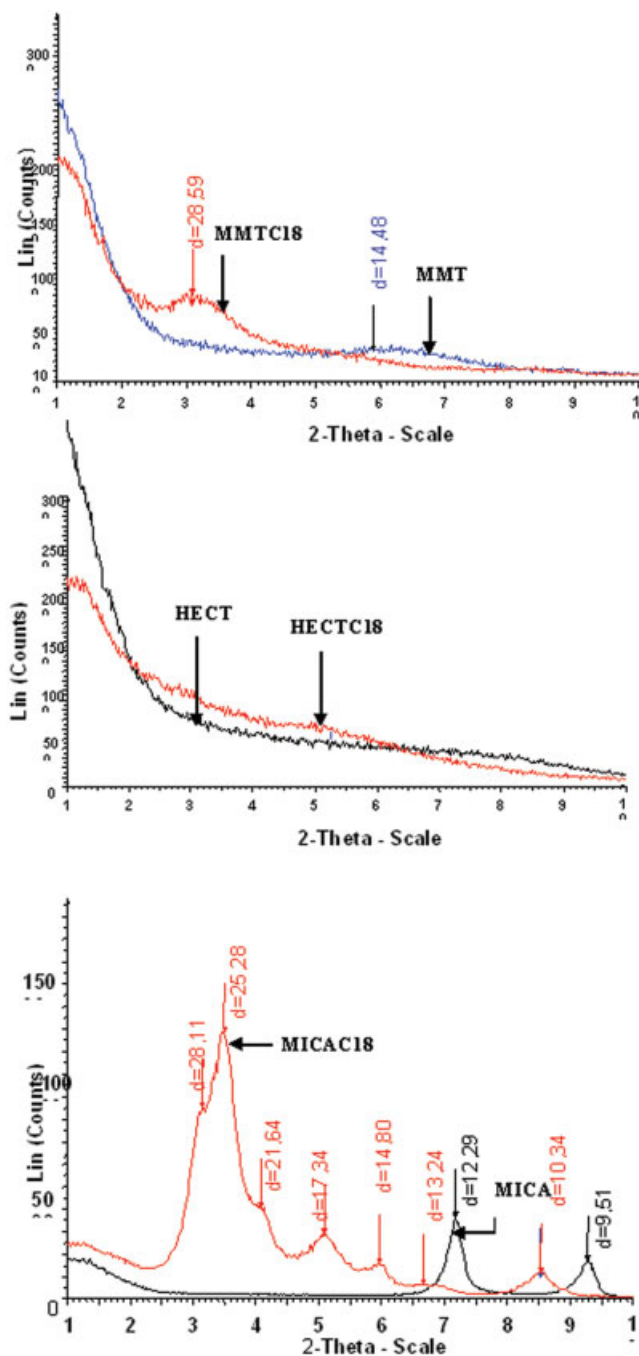


**Figure 3** XRD Spectra of three lamellar silicates before and after modification by octadecylammonium ions: (a) MMT, (b) HECT, and (c) MICA. [Color figure can be viewed in the online issue, which is available at [www.interscience.wiley.com](http://www.interscience.wiley.com).]

philic modification is not very homogeneous for the mica, leading to the presence of well-intercalated tactoids with varying *d*-spacing. Taking into account of the crystalline organization lack for pristine hectorite, it is impossible to characterize the intercalation of organic chains between hectorite platelets by WAXD.

In Figure 4, the thermogravimetric analysis (TGA) reveals several peaks linked to a volatile departure.

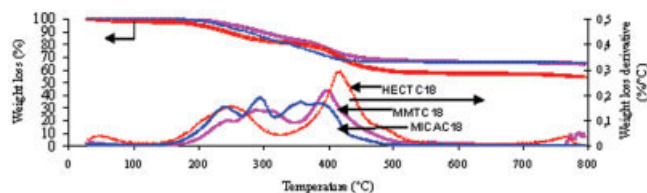


**Figure 4** Weight loss and weight loss derivative of organoclays after washing: MMTC18, HECTC18, and MICAC18. [Color figure can be viewed in the online issue, which is available at [www.interscience.wiley.com](http://www.interscience.wiley.com).]

The low-temperature peak, located between 40 and 70°C, is associated to the vaporization of free water and water bonded to the cations by hydrogen bonds.<sup>24</sup> The following decompositions are related to alkylammonium ions. It was shown previously,<sup>16</sup> that the first decomposition step is due to adsorbed cations. In fact, after the cationic exchange, some ions remain adsorbed on hydroxyl groups on platelets edges and are not intercalated between the nanoplatelets. The thermal decomposition takes place in the 200–350°C range. The well intercalated modifying ions show a higher thermal stability and the decomposition temperature included between 350 and 500°C depends on interactions kinds of organic groups with the platelet surface.<sup>21,22</sup> At temperatures higher than 700°C, the dehydroxylation of the silicates takes place. Thus the organophilic clays display organic chains both inside galleries as intercalated species and outside platelets as adsorbed species. This later category could be a wettability aid of nanofillers for being introduced into organic medium. The ratio of organic species is reported in Table III. The cationic exchange capacity was measured from the amount of intercalated ions determined after careful washing and the values are 90, 120, and 70 meq/100 g for MMT, HECT and MICA respectively. Hectorite is the silicate showing the highest intercalated ions ratio inside galleries.

From DSC experiments, an endothermal peak ( $\Delta H_d$ ) at a melting temperature  $T_d$  is put into evidence during heating and can be associated with an alkylammonium chain order/disorder transition corresponding to a liquid crystal/liquid state transition. These values (reported in Table IV) show that for a same surface

**TABLE IV**  
Determination ( $v = 10$  K/min) of Melting Enthalpy for Organophilic Clays ( $\Delta H_d$ ) Related to Order–Disorder Transition Temperature ( $T_d$ ) and Pseudocrystallinity Rate ( $\chi$ ) of Organic Chains by Using DSC

Parameters	MMTC18	HECTC18	MICAC18
$T_d$ (°C)	64	37	93
$\Delta H_d$ ions (J/g)	49	23	106
$\chi$ (%)	17	7	29

**TABLE V**  
Determination of Interlayer Distance ( $d_{001}$ , Å) of Alkylammonium-Exchanged Clays by XRD and Comparison with the Theoretical Extended Chain Length and the Tilt Angle  $\alpha$

Sample	$d_{001}$ spacing (Å)	$l_t$ (Å)	Tilt angle $\alpha$ (°)
MMTC18	28.6	24.3	35.5
HECTC18	–	24.3	–
MICAC18	25.3	24.3	32.3

treatment, the organization of alkyl chains differs with the silicate nature. A pseudocrystallinity rate  $\chi$ , reported in Table IV, can be deduced from the heat of the melting peak with respect to the polyethylene crystal melting heat, i.e., 280 J/g. In accordance with X-ray analyses, MICAC18 is the more organized silicate with a pseudocrystallinity rate of 29%, associated to the highest order/disorder transition. On the other hand, HECTC18, which shows no diffraction peak significant of an intercalated structure on long distances, presents the lowest crystallinity ratio (7%) associated to the lowest transition temperature. The MMTC18 shows an intermediate crystalline behavior. To evaluate the conformation of the chains in the clay galleries, we have reported the theoretical length when the alkyl chains adopt a trans–trans conformation. The theoretical extended chain length,  $l_t$ , can be calculated as proposed by Lagaly<sup>25</sup>

$$l_t(\text{Å}) = 1.265(n_c - 1) + 3 \quad (3)$$

where  $(n_c - 1)$  is the number of methylene groups in the alkyl chain, 1.265 Å is the contribution due to the  $-\text{CH}_2-$  chain segments by assuming that the chains adopt an all-trans configuration, and we add the dimension of the methyl end group (3 Å). The tilt angle  $\alpha$ , can be calculated as follows

$$\alpha = \arcsin(d_{001} - d'_{001})/l_t \quad (4)$$

where  $d_{001}$  and  $d'_{001}$  are the  $d$ -spacing of modified and pure clays, respectively.

Results reported in Table V for MMTC18 and MICAC18 reveal that the basal spacing is very close to the theoretical extended chain length, which suggests that the chains adopt a paraffin-like structure in a tilted arrangement with respect to the silicate surface.

So, we have three silicates, one natural and two synthetic with very distinct cationic exchange capacities. After organophilic modification, HECTC18 does not show any repetitive structure (impossible to determine a regular  $d$ -spacing, very low crystallinity ratio) but presents the highest amount of exchanged organic ions (38 wt %), leading to a very hydrophobic

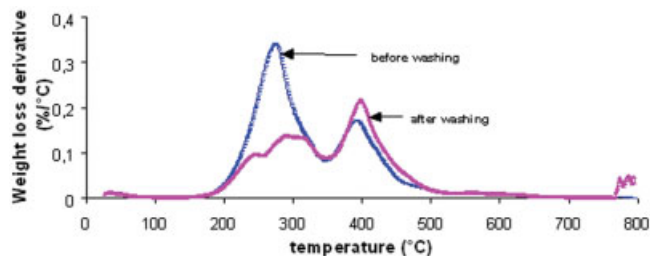


**Figure 5** Weight loss derivative of MMTC18 as a function of temperature before and after washing. [Color figure can be viewed in the online issue, which is available at [www.interscience.wiley.com](http://www.interscience.wiley.com).]

silicate. On the other hand, MICA shows a very ordered host structure with a high purity degree. After the cationic exchange, MICAC18 has a very hydrophobic surface similar to a polyolefin one and keeps a very crystalline character (silicate with the highest crystallinity ratio, i.e., 29%) while showing an intercalated structure with a  $d$ -spacing distribution. MMTC18 presents an intermediate behavior: less crystalline than MICAC18 but more than HECTC18, with a hydrophobic surface but keeping the highest polar component.

With the same kind of exchanged ions, we have generated three organophilic silicates with different surface properties, a variable crystallinity, a different structuration depending on their chemical composition, their exchange capacity, and their geometrical characteristics.

### Influence of the washing after exchange

The washing step in the cationic exchange process has an important effect because it allows to obtain well-structured layers by removing the physisorbed octadecylammonium ions and by keeping only the intercalated ions in the galleries. The weight loss derivative,  $dm/dT$ , as a function of the temperature is reported in Figure 5, showed after the washing step, a decrease in amount of the physisorbed ions that was bound to the clay by Van der Waals bonds, while keeping the same quantity of intercalated ions (Table VI). The washed organoclay is likely to be more suit-

**TABLE VI**  
Effect of Washing on the Physisorbed and Intercalated Ions Ratio Determined by TGA on Three Organophilic Silicates

Samples	Before washing		After six washings	
	Physisorbed ions	Intercalated ions	Physisorbed ions	Intercalated ions
MMTC18	20.6	18.3	12.7	18.3
HECTC18	18.5	22.7	15.4	22.4
MICAC18	21.7	14.5	19.7	14.3

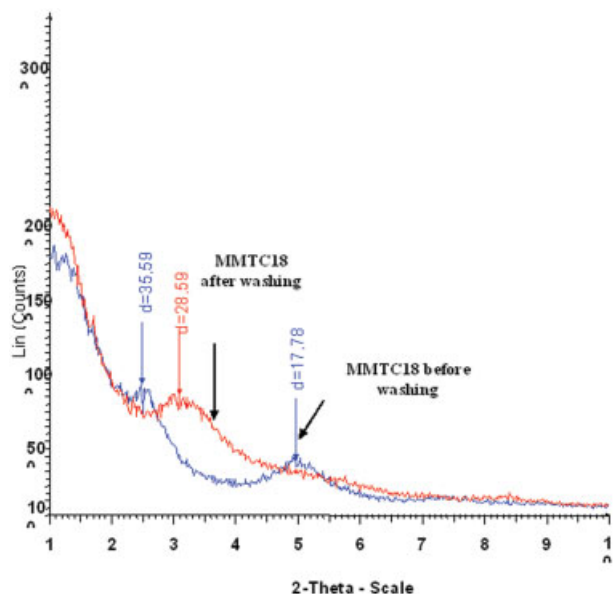


**Figure 6** XRD spectra of MMT C18 organoclay before and after washing. [Color figure can be viewed in the online issue, which is available at [www.interscience.wiley.com](http://www.interscience.wiley.com).]

able for incorporation with a polymer melt in an extruder or during curing of a thermoset without being degraded. So the washing step allows to improve the silicate thermal stability. The washing step also modifies the structure of silicates by giving a new mobility to alkyl chains and a chain rearrangement possibility. After washing, the *d*-spacing of MMTC18 decreased as shown in Figure 6. This variation of the *d*-spacing after washing was also observed by Klapyta et al.<sup>26</sup> So the washing step allows to modulate the modified silicate/organic medium interfaces by generating either very hydrophobic nanofillers, keeping physisorbed ions, or more thermally stable nanofillers, keeping only alkyl chains confined between layers, and removing physisorbed ions.

**Silicate/monomer interactions**

**Interlamellar swelling**

To evaluate simply silicate/organic medium interactions, a first experiment consists in measuring the swelling of silicate in monomer at the interplatelet scale. We have performed these experiments on MICAC18, which presents a well intercalated structure, whose interlamellar swelling is easy to follow by WAXD analysis. After its introduction into the DGEBA or D2000 monomers, we observe an increase of interlamellar *d*-spacing that reveals diffusion of monomers between the layers. However, the swelling of MICAC18 in amine is more favorable than in DGEBA and leads to a better state of dispersion since a interlamellar swelling of 34 Å was determined in

amine against only 10 Å in epoxy. As the surface treatment is similar for the three clays, it is reasonable to consider that the interactions between organophilic silicates and amine are similar for the two others clays (MMTC18 and HECTC18).

**Evidence of gel-like behavior**

*Newtonian behavior of monomers.* Without silicate, the epoxy prepolymer has a typical liquid like behavior at 80°C. The loss and storage moduli vary with angular frequency following power laws, with power law indexes of 1 and 2 respectively, (Fig. 7). The loss angle value of the DGEBA is 90° in the whole range of angular frequencies considered. The same liquid-like behavior was observed with Jeffamine D2000 at 80°C.

**Viscoelastic behavior of gels**

The rheological behavior of silicate suspensions dispersed handly in DGEBA and Jeffamine monomers was studied at a small deformation in the linear viscoelastic range. Physical gels are identified by the existence of a significant frequency independent storage modulus and a low phase angle value, usually inferior to 25°. Figure 8 reports the rheological behavior of a 5 phr HECTC18 suspension in DGEBA. The storage modulus (*G'*) of this suspension was around 8700 Pa, almost frequency independent and the loss angle ( $\delta$ ) was less than 25°. In this case, the gel was not a purely elastic solid because the loss angle was not equal to zero as for a hookean solid.

Gels are formed and remain stable for low applied stress as shown in Table VII, where the gel storage modulus (*G'*) and loss angle ( $\delta$ ) are reported for the different suspensions. Montmorillonite with a 5 phr ratio, with or without surface treatment, forms easily physical gels in both monomers, DGEBA or JEFFAMINE. For MMT, it seems that only the aspect ratio is the determining factor to form a gel. There is no effect

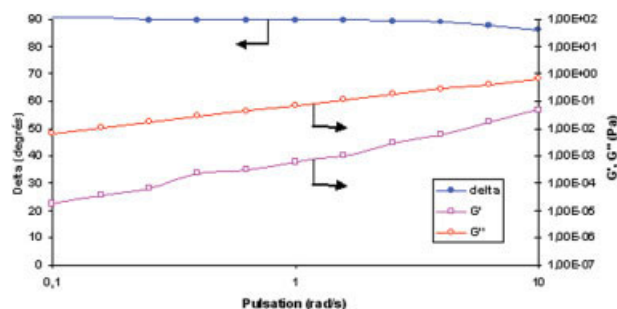


**Figure 7** Storage modulus *G'* (□), loss modulus (○) and loss angle (●) variations with angular frequency of DGEBA prepolymer with an oscillating stress of 0.1 Pa at 80°C. [Color figure can be viewed in the online issue, which is available at [www.interscience.wiley.com](http://www.interscience.wiley.com).]



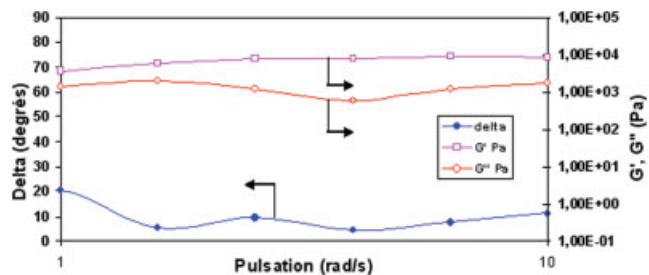


**Figure 8** Storage modulus  $G'$  ( $\square$ ), loss modulus ( $\circ$ ) and loss angle ( $\bullet$ ) variations with angular frequency of a 5 phr HECTC18/DGEBA with an oscillating stress of 0.1 Pa at 80°C. [Color figure can be viewed in the online issue, which is available at [www.interscience.wiley.com](http://www.interscience.wiley.com).]

of neither the surface treatment nor the generated interactions in organic medium considered. On the other side, for hectorite, the surface treatment seems to have an influence on the gel structuration since the gel storage modulus decreases both in epoxy and in amine when the modified hectorite is added. We can think that the surface treatment improves the dispersion state and leads to a more swollen and so less strong physical gel. The last silicate, MICA, shows a specific behavior: (i) when its surface is rather hydrophilic, MICA forms a gel only in the DGEBA monomer which is more polar; (ii) when its surface is rendered hydrophobic, MICAC18 forms a gel only in the JEFFAMINE monomer. It seems that the interactions between mica/DGEBA are better with an hydrophilic silicate surface, whereas in the D2000 monomer, the mica surface treatment is necessary.

However, it results from these rheological analysis that all the silicates, modified or not, in both monomers form very strong physical gels with a very high storage modulus. Only MICAC18 in JEFFAMINE form a weak gel, showing a storage modulus of 20 Pa.

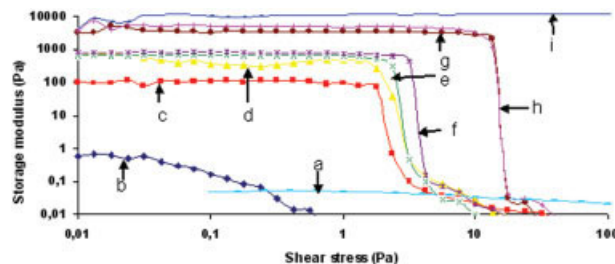


**Figure 9** Storage modulus variation at 80°C and at 10 rad/s during stress sweeps for HECTC18/DGEBA suspensions for different amounts of HECTC18: (a) 0, (b) 0.25, (c) 0.5, (d) 1, (e) 2, (f) 3, (g) 4, (h) 5, and (i) 30 phr. [Color figure can be viewed in the online issue, which is available at [www.interscience.wiley.com](http://www.interscience.wiley.com).]

After shearing at a critical stress (Table VII), the gel/sol transition occurs and the resulting fluid shows a high apparent viscosity significant of strong interactions between silicate and monomer. We have put into evidence that the storage modulus of the gel is directly proportional to the stress at break when suspension ratio or the steering time were varied. This means that whatever the strength of the gel is, the deconstruction of the gel for various stress at break, a similar shear deformation at a macroscopic scale is needed. We can conclude that a different nanostructuration of silicates in the monomers is responsible for the gel strength and this nanostructuration is only dependent on geometric characteristics of silicate since physicochemistry interactions are similar.

To characterize more precisely the gel formation, the modulus evolution was measured with varying the modified hectorite amount introduced in DGEBA as a function of shear stress. Three typical regions are observed in Figure 9. The first one, corresponding to the gel formation, is characterized by a high and con-

**TABLE VII**  
Storage Modulus, Stress at Break and Relative Viscosity at 1000 s<sup>-1</sup> Measured on a 5 phr Clay Suspension in DGEBA and JEFFAMINE D2000 Monomers at 80°C

Dispersion medium	Silicates	Storage Modulus in the gel state (Pa)	Stress at break $\tau_b$ (Pa)	Relative viscosity
DGEBA	None	Sol	Sol	1
	MMT	450	3	1.17
	HECT	28,000	150	1.11
	MICA	100	0.09	1.15
	MMTC18	635	4.19	1.34
	HECTC18	8700	16.5	1.26
	MICAC18	1.56	Sol	1.49
	None	Sol	Sol	1
	MMT	90	0.5	1.16
	HECT	25,000	90	1.13
	MICA	10	Sol	1.19
	MMTC18	1400	10	1.28
Jeffamine D2000	HECTC18	3800	20	1.13
	MICAC18	20	0.08	3.03

stant storage modulus: the material is similar to an elastic solid. The second area corresponds to the gel-sol transition and the storage modulus decreases quickly when the gel is broken and the material is similar to a viscoelastic fluid. Eventually, the third region is characteristic of a liquid with a very low value of storage modulus tending to zero. At low organoclay ratio, less than 0.5 phr, silicates do not form gel in the monomer. From 0.5 phr, a significant modulus is detected characteristic of the silicate connection in the DGEBA monomer. Consequently, the percolation ratio is situated around 0.5 phr silicate. Below this value, the silicate amount is not enough to form a silicate percolating network. Above this value, higher the silicate amount is, stronger the physical gel is. And more than 30 phr, the suspension does not present anymore gel/sol mechanical transition, even for high stresses; the suspension remains a gel and cannot flow whatever the applied stress is. Although there was not a strict anticorrelation, we can see as main trend that the highest viscosities are obtained with the lowest gel strength, representative of a swollen structure, contributing to the increase of the apparent volume fraction of filler and thus of the viscosity (Fig. 10). The effect of diffusion about the morphology of 5 phr HECTC18/DGEBA suspension was studied. The result shows that the intensity of the peaks increases with time (Fig. 11). Time let the diffusion of prepolymer in the interlayer or intergallery spacing of the silicate.<sup>29</sup>

### CONCLUSIONS

The performance of nanocomposites is not only related to the nature of their components but also to the reinforcing mechanism of fillers that are bound to their dispersion state. In a first time, we have introduced the lamellar silicates in precursors of an epoxy/amine network to evaluate the interactions and the

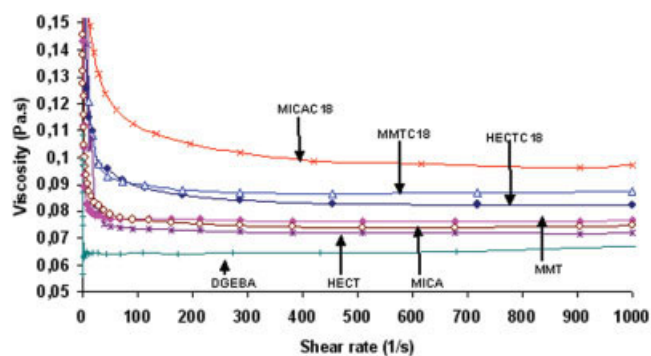


**Figure 10** Effect of the shear rate on the viscosity of a 5 phr suspension in DGEBA at 80°C. [Color figure can be viewed in the online issue, which is available at [www.interscience.wiley.com](http://www.interscience.wiley.com).]

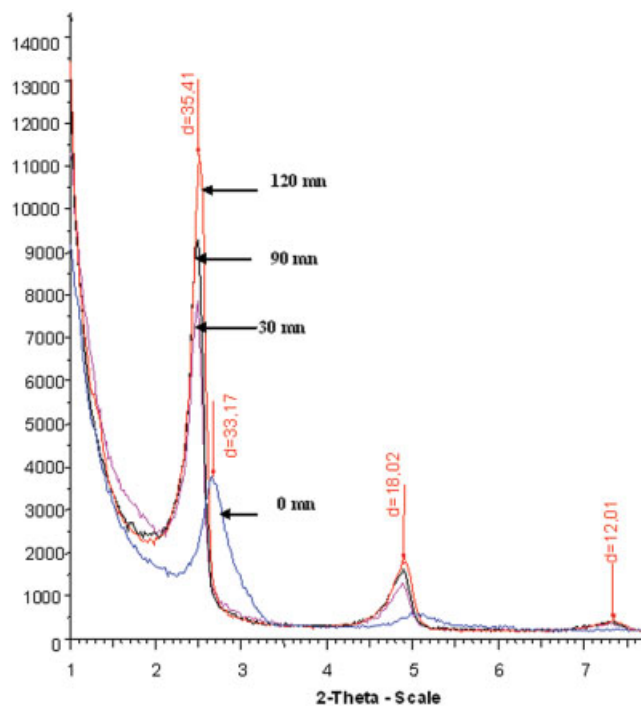


**Figure 11** Effect of the diffusion time on XRD spectra performed on MICAC18 (5phr)/DGEBA suspension at 80°C. [Color figure can be viewed in the online issue, which is available at [www.interscience.wiley.com](http://www.interscience.wiley.com).]

structuration of these lamellar silicates in a viscous organic medium before curing. The nanostructuration of these suspensions is strongly dependent on the host structure and surface properties of nanofillers. These physicochemistry parameters must be carefully chosen to reach an optimum dispersion state.

In this work, montmorillonite, mica, and hectorite, which are three lamellar silicates showing different aspect ratios, were modified by the same surface treatment, i.e., octadecylammonium ions by cationic exchange. By tailoring both the modifying ions/clay ratio (responsible for the number of organic cations that can be intercalated into clay galleries and the number of washings that governs the quantity of physisorbed alkylammonium ions and the thermal stability), different silicate/matrix interfaces could be designed.

After modification, HECTC18 has the highest organic ratio and shows a very hydrophobic surface without platelets crystalline organization. On the other side, MICAC18 is very crystalline with very intercalated and well exchanged platelets. MMTC18 has an intermediate behavior: less organized and less hydrophobic than MICAC18.

Rheological study demonstrates that organoclay suspensions in organic medium form physical gels when no shear is applied. Gel strength and apparent viscosity measurements suggest the existence of different nanostructuration depending on the silicates'

aspect ratio and chemical modification that govern the physical interactions between silicates and the epoxy precursors of networks.

## References

1. Becker, O.; Ceng, Y. B.; Varley, J. R.; Simon, G. P. *Macromolecules* 2003, 36, 1616.
2. Ray, S. S.; Okamoto, M. *Prog Polym Sci* 2003, 28, 1539.
3. Gilman, J. W. *Appl Clay Sci* 1999, 15, 31.
4. Nah, C.; Kim, H. D.; Choi, S. S. *Polym Adv Technol* 2002, 13, 649.
5. Hussain, M.; Varley, R. J.; Mathys, Z.; Cheng, Y. B.; Simon, G. P. *J Appl Polym Sci* 2004, 91, 1233.
6. Becker, O.; Varley, R. J.; Simon, G. P. *Eur Polym J* 2004, 40, 187.
7. Lagaly, G.; Malberg, R. *Colloids Surf* 1990, 49, 11.
8. Gherardi, B. Ph.D. Dissertation, University of Orléans, France, 1998.
9. Luckham, P. F.; Rossi, S. *Adv Colloid Interface Sci* 1999, 82, 43.
10. Gherardi, B.; Tahani, A.; Levitz, P.; Bergaya, F. *Appl Clay Sci* 1996, 11, 163.
11. Moraru, N.V. *Appl Clay Sci* 2001, 19, 11.
12. Burgentzlé, D.; Duchet, J.; Gerard, J. F.; Jupin, A.; Fillon, B. *J Colloid Interface Sci* 2004, 278, 26.
13. Jordan, J. W. *J Phys Colloid Chem* 1949, 53, 294.
14. Krishnamoorti, R.; Yurekli, Y. *J Colloid Interface Sci* 2001, 6, 464.
15. Le Pluart, L.; Duchet, J.; Sautereau, H.; Halley, H. P.; Gérard, J. F. *Appl Clay Sci* 2004, 25, 207.
16. Le Pluart, L.; Duchet, J.; Sautereau, H.; Gérard, J. F. *J Adhes* 2002, 78, 645.
17. Sebaa, M.; Servens, C.; Pouyet, J. *J Appl Polym Sci* 1992, 45, 1049.
18. Bradley, G. W.; Brown, G. Mineralogical Society: London, 1980.
19. Hoffmann, B.; Kressler, J.; Stoppelman, G.; Friedrich, C.; Kim, G. M. *Colloid Polym Sci* 2000, 278, 629.
20. Kormmann, X.; Lindberg, H.; Berglund, L. A. *Polymer* 2001, 42, 4493.
21. Xie, W.; Gao, Z.; Liu, K.; Pan, W. P.; Vaia, R.; Hunter, G.; Singh, A. *Thermochim Acta* 2001, 367, 339.
22. Xie, W.; Xie, R.; Pan, W. P.; Hunter, G.; Koen, B.; Vaia, R. *Chem Mater* 2002, 14, 4837.
23. Owens, D. K.; Wendt, R. C. *J Appl Polym Sci* 1969, 13, 1741.
24. Xie, W.; Gao, Z.; Pan, W. P.; Hunter, G.; Singh, A.; Vaia, R. *Chem Mater* 2001, 13, 2979.
25. Lagaly, G. *Solid State Ionics* 1986, 22, 43.
26. Klapayta, Z.; Fujita, T.; Lyi, N. *Appl Clay Sci* 2001, 19, 5.
27. Terech, P.; Pasquier, D.; Bordas, V.; Rossat, C. *Langmuir* 2000, 16, 4485.
28. Mercurio, D. J.; Khan, S. A.; Spontak, R. J. *Rheol Acta* 2001, 40, 30.
29. Theodore, M.; Deam, D.; Obore, A.; Nyairo, E. *Polym Prepr* 2004, 45, 863.